SCIENTIFIC REPORTS

OPEN

Term rules for simple metal clusters

Daisuke Yoshida[1] & Hannes Raebiger[1,2]

Received: 15 July 2015
Accepted: 29 September 2015
Published: 26 October 2015

Hund's term rules are only valid for isolated atoms, but have no generalization for molecules or clusters of several atoms. We present a benchmark calculation of Al_2 and Al_3, for which we find the high and low-spin ground states $^3\Pi_u$ and $^2A_1'$, respectively. We show that the relative stabilities of all the molecular terms of Al_2 and Al_3 can be described by simple rules pertaining to bonding structures and symmetries, which serve as guiding principles to determine ground state terms of arbitrary multi-atom clusters.

The ground state terms (spin and angular momenta) of isolated atoms are determined by Hund's rules[1], which are explained by the lowering of the electronuclear attraction energy[2–5]. For molecules and clusters, such term rules do not exist. Group theory allows us to determine the possible $^{2S+1}\Xi$ molecular terms, where S denotes the total spin and Ξ the symmetry species, but there is no systematic way to figure out which of these is the ground state. Direct experimental observation or quantum chemical total energy calculation is only available for a few prototype systems.

Hund's first rule of maximum spin multiplicity holds for many organic molecules[6–8], but not all[9]. Diatomic molecules on the other hand, tend to have spin singlet ground states with the exception of O_2 and B_2 (see e.g. refs 10–19 for diatomic molecules of main group elements). These molecules tend to have ground states that minimize the internuclear bond length, which may be associated with a lowering of the electronuclear attraction energy, but whether or not such discussion generalizes to metallic clusters remains unknown. Moreover, recent attempts to generalize Hund's rules for molecules[8,20] or clusters[21–23] only focus on a spin multiplicity rule, and trends or rules for Ξ (symmetry) terms remain completely uncharted territory.

Simple Al clusters emerge as the ideal model system to study term rules. Bulk Al is paramagnetic, but in low dimensional structures Al atoms may spontaneously align their spins. For example, strained quasi-1D chains of Al may exhibit ferromagnetism[24,25], and Al_n clusters with even $n = 2$, 4, 6, 8 have spin-triplet ground states[21,26–29]. Al_3 on the other hand has spin-doublet (low-spin) and spin-quadruplet (high-spin) configurations, but which one of these is the ground state remains unresolved[28,30–33]. The present benchmark study confirms that Al_2 has the $^3\Pi_u$ high-spin ground state and unambiguously shows that Al_3 has the low-spin $^2A_1'$ ground state. The Al_2 high-spin state is stabilized by Fermi correlation, which is not overcome by Coulomb correlation that tends to increase the stability of low-spin terms. For Al_3, however, the high-spin term has a symmetry broken geometry that preempts effective Coulomb correlation from taking place, thus un-stabilizing the high-spin term. Such symmetry lowering can debilitate high-spin terms of any multi-atom system. Moreover, fear each spin state, we find a simple rule for the Ξ terms. The Ξ term with least node wavefunction is most stable, and for terms with equal number of nodes, the one with most bonds is most stable. Notice that for diatomic molecules, Ξ is the angular momentum $\left(\Xi = \Lambda^{(\pm)}_{(g/u)}\right)$ along the internuclear axis, which can be either minimized or maximized by this rule.

Results

Al_2 has five stationary states, $^1\Sigma_g^+$, $^1\Pi_u$, $^1\Delta_g$, $^3\Pi_u$ and $^3\Sigma_g^-$, corresponding to the occupation of different molecular orbitals by two $3p$ electrons. Al_3 has three stationary states, $^2A_1'$, $^4A_2$ and $^4B_1$, corresponding

[1]Department of Physics, Yokohama National University, Yokohama, Japan. [2]Centro de Ciências Naturais e Humanas, Universidade Federal do ABC, Santo André, SP, Brazil. Correspondence and requests for materials should be addressed to H.R. (email: hannes@ynu.ac.jp)

Al_2	HF		CAS(6, 18)		CAS(6, 26)				
	E	*r*	*E*	*r*	*E*	*r*			
$^3\Pi_u$	−483.7824(0)	2.770	−483.8939(23)	2.714	−483.9082(13)	2.729			
$^3\Sigma_g^-$	−483.7700(2)	2.544	−483.8892(27)	2.474	−483.9064(16)	2.501			
$^1\Sigma_g^+$	−483.7647(1)	2.996	−483.8830(21)	2.972	−483.8980(12)	2.980			
$^1\Pi_u$	−483.7627(1)[a]	2.754	−483.8775(14)	2.745	−483.8925(8)	2.749			
$^1\Delta_g$	−483.7369(6)	2.619	−483.8760(28)	2.528	−483.8915(15)	2.556			
Al_3	HF			CAS(9, 12)			CAS(9, 18)		
	E	*r*	*θ*	*E*	*r*	*θ*	*E*	*r*	*θ*
$^2A_1'$	−725.6780(30)	2.607	60.0°	−725.8100(74)	2.567	60.0°	−725.8655(73)	2.530	60.0°
$^4A_2$	−725.7007(27)	2.651	71.7°	−725.7962(63)	2.620	69.6°	−725.8554(64)	2.591	70.0°
$^4B_1$	−725.6995(25)	2.868	54.2°	−725.7969(63)	2.784	55.8°	−725.8496(67)	2.760	55.6°

Table 1. Total energies and equilibrium structures of Al_2 and Al_3. Total energies *E* are given in hartree atomic unit (a.u), and Al-Al bond *r* lengths in Å. For Al_3 *r* is the length of either leg of an isosceles triangle with vertex angle *θ*. Values in parenthesis are maximum errors within the virial theorem. [a]CAS(2, 2) calculation using doubly degenerate configurations in $(3p\pi_u^+)^1(3p\pi_u^-)^1$.

to the occupation of different molecular orbitals by three 3*p* electrons. Their equilibrium nuclear geometries and corresponding total energies *E* are shown in Table 1. Hartree-Fock (HF) calculation predicts Al_2 and Al_3 to have $^3\Pi_u$ and $^4A_2$ high-spin ground states, respectively. Inclusion of Coulomb correlation by CAS-SCF (see Methods) maintains the high-spin ground state of Al_2, but stabilizes the $^2A_1'$ low-spin ground state of Al_3. At the same time, high-spin terms of Al_2 ($^3\Pi_u$, $^3\Sigma_g^-$) and Al_3 ($^4A_2$, $^4B_1$) become nearly degenerate; the energy difference between them is smaller than 0.01 a.u. The $^3\Pi_u$ ground state for Al_2 is consistent with experiment[34], and our prediction of the $^2A_1'$ ground state for Al_3 is corroborated by the Stern-Gerlach experiment[30]. More importantly, the ground state of Al_2 is consistent with both Hund's first and second rules, whereas Al_3 violates both of them.

Potential energy components. Traditionally, Hund's rules have been interpreted as an energy gain due to the inter-electron repulsion potential energy V_{ee}[35–37], and more recently as an energy gain due to the electronuclear attraction V_{en}[2,4,5,7,8]. In order to analyze whether or not similar energy lowering mechanisms can be invoked for Al_2 and Al_3, we decompose the total energies given in Table 1 into potential energy components shown in Fig. 1. In both HF (dashed lines) and CAS-SCF (solid lines) calculations for each stationary state of Al_2 and Al_3, repulsion terms V_{ee} (red lines) and V_{nn} (blue lines; inter-nuclear repulsion) are positive and the attraction term V_{en} (purple lines) is negative. The total energies *E* of Al_2 and Al_3 calculated by CAS-SCF always lie lower than those calculated by HF. For both Al_2 and Al_3, upon inclusion of Coulomb correlation by CAS(6, 26) and CAS(9, 18), respectively, the individual potential energy components V_{en}, V_{ee} and V_{nn} composing *V* change as follows: both V_{ee} and V_{nn} increase and V_{en} decreases. The correlation energies $E^c = E^{CAS} - E^{HF}$, along with V^c, V_{en}^c, V_{ee}^c, and V_{nn}^c, defined similarly, are unique to each molecular term; $E^c < 0$ always, and for the components we find $V_{en}^c < 0$, $V_{ee}^c > 0$, and $V_{nn}^c > 0$.

For Al_2, both HF and CAS-SCF predict

$$E^{\mathrm{HF/CAS}}(^3\Pi_u) < E^{\mathrm{HF/CAS}}\left(^3\Sigma_g^-\right) < E^{\mathrm{HF/CAS}}\left(^1\Sigma_g^+\right) < E^{\mathrm{HF/CAS}}(^1\Pi_u) < E\left(^1\Delta_g\right). \quad (1)$$

The correlation energies, however, exhibit the different trend

$$E^c\left(^1\Delta_g\right) < E^c\left(^3\Sigma_g^-\right) < E^c\left(^1\Sigma_g^+\right) < E^c(^1\Pi_u) < E^c(^3\Pi_u) \quad (2)$$

making the excitation energies smaller. For Al_3, HF predicts

$$E^{\mathrm{HF}}(^4A_2) < E^{\mathrm{HF}}(^4B_1) < E^{\mathrm{HF}}(^2A_1') \quad (3)$$

and CAS-SCF predicts

$$E^{\mathrm{CAS}}(^2A_1') < E^{\mathrm{CAS}}(^4A_2) < E^{\mathrm{CAS}}(^4B_1) \quad (4)$$

i.e. the level ordering is altered by correlation effects. For correlation energies we find

$$E^c(^2A_1') < E^c(^4A_2) < E^c(^4B_1). \quad (5)$$

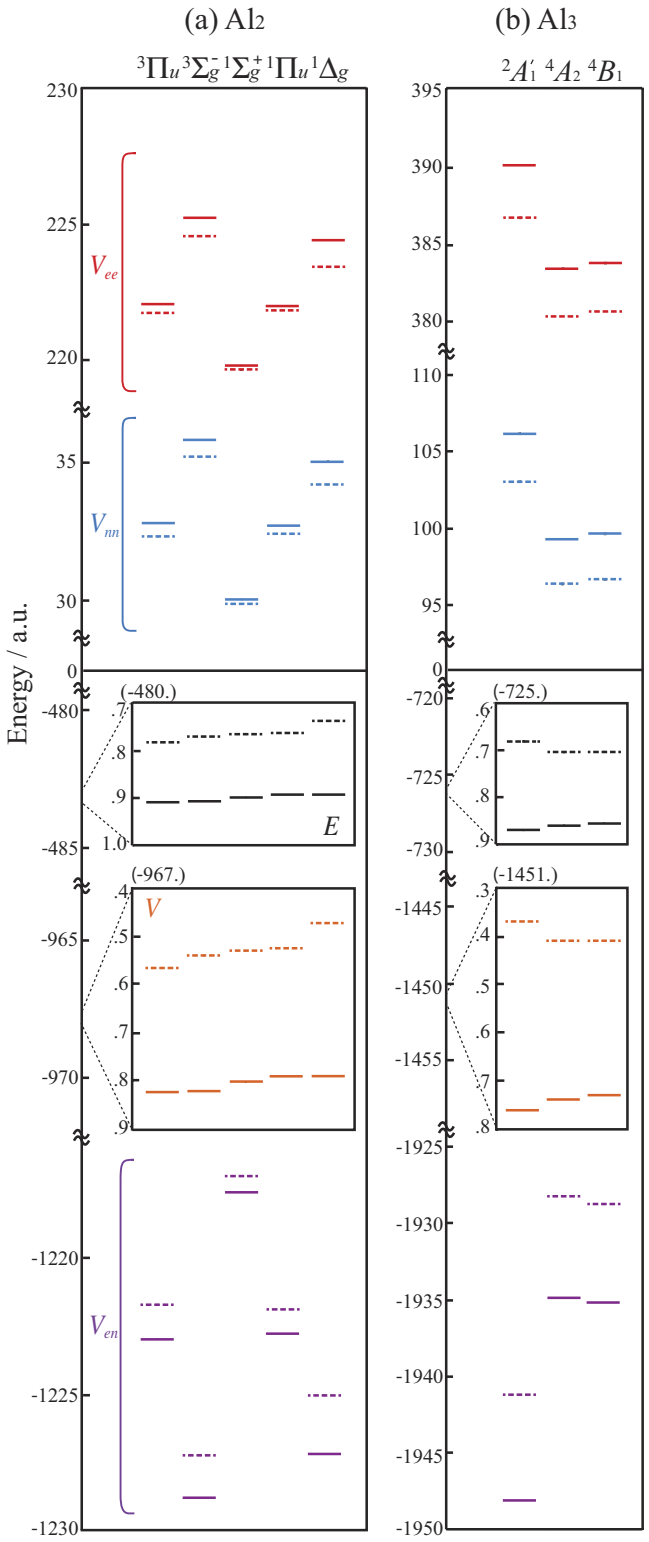

Figure 1. Energy components for each equilibrium state of Al_2 and Al_3. HF, CAS(6, 26) for Al_2 and CAS(9, 18) for Al_3 levels are dashed lines and solid lines, respectively. E (black), V (orange), V_{ee} (red), V_{nn} (blue), and V_{en} (purple) are given in hartree atomic units.

For both Al_2 and Al_3, the strongest correlation effect, i.e. greatest correlation energy E^c, is observed for the $^1\Delta_g$ and $^2A_1'$ low-spin terms, respectively. For Al_3, this correlation effect is strong enough to alter the level ordering of the molecular terms, but for Al_2 not. Thus, the relative stability of the Al_2 molecular

Al_2		Al_3	
$^3\Pi_u$	$[3s]3p\sigma_g^1 3p\pi_u^1$	$^2A_1'$	$[3s]3p\pi\,(a_2'')^2 3p\sigma\,(a_1')^1$
$^3\Sigma_g^-$	$[3s]\,3p\pi_u^2$	$^4A_2$	$[3s]3p\pi(b1)^1 3p\sigma(a1)^1 3p\sigma(b2)^1$
$^1\Sigma_g^+$	$[3s]\,3p\sigma_g^2$	$^4B_1$	$[3s]3p\pi(b1)^1 3p\sigma(a1)^1 3p\sigma(a1)^1$
$^1\Pi_u$	$[3s]\,3p\sigma_g^1 3p\pi_u^1$		
$^1\Delta_g$	$[3s]\,3p\pi_u^2$		

Table 2. Electronic configurations of valence electrons of Al_2 and Al_3. $[3s]$ represents the configurations of $3s$ electrons; In Al_2, $[3s]=3s\sigma_g^2 3s\sigma_u^2$, In Al_3, $[3s] = 3s\sigma\,(a_1')^2 3s\sigma\,(e')^4$ for $^2A_1'$, and $[3s]=3s\sigma(a_1)^2 3s\sigma(a_1)^2 3s\sigma(b_2)^2$ for $^4A_2$ and $^4B_1$.

terms can be discussed based on Fermi correlation (Pauli's exclusion principle) and HF calculations, but for Al_3, Coulomb correlation included by CAS-SCF is crucial for the description of molecular terms.

For Al_2, Hund's first and second rules predict

$$E\,(^3\Pi_u) < E\left(^3\Sigma_g^-\right) < E\left(^1\Delta_g\right) < E\,(^1\Pi_u) < E\left(^1\Sigma_g^+\right), \tag{6}$$

which is valid only for the spin-triplet terms. The spin-singlet terms exhibit an opposite trend to Hund's second rule. Term stabilities have earlier been interpreted by either V_{ee}[35–37] or V_{en}[2,4,5,7,8], which imply that total energy differences are dominated by one potential energy component V_i($i = ee$, en, or nn), i.e., the total energy should follow the trend of this dominant V_i. Figure 1, however, shows that

$$(\pm)\,V_i\left(^3\Sigma_g^-\right) < (\pm)\,V_i\left(^1\Delta_g\right) < (\pm)\,V_i(\,^3\Pi_u) < (\pm)\,V_i(\,^1\Pi_u) < (\pm)\,V_i\left(^1\Sigma_g^+\right), \tag{7}$$

which is different to Eq. (1). Here the + sign corresponds to $i = en$, and the − sign to $i = ee$ and $i = nn$. Clearly total energy trends do not follow any one particular potential energy component. Although the highest spin multiplicity (Hund's first) rule does not follow any of the potential energy components V_{en}, V_{ee}, and V_{nn}, the Ξ terms, when observed for spin-triplet and spin-singlet states individually, exhibit the following trends

$$(\mp)\,V_i(\,^3\Pi_u) < (\mp)\,V_i\left(^3\Sigma_g^-\right) \tag{8a}$$

$$(\pm)\,V_i\left(^1\Sigma_g^+\right) < (\pm)\,V_i(\,^1\Pi_u) < (\pm)\,V_i\left(^1\Delta_g\right). \tag{8b}$$

Note that Eq. (8a) has the opposite sign convention to Eqs (7) and (8b). Thus, for a given spin multiplicity, the potential energy components follow the same trend as total energies, but the sign may vary case by case!

Fermi correlation and bond structure. Since clear term rules cannot be described based on the individual energy components discussed above, we turn our attention to the bond structures given in Table 2 for each molecular term. For Al_2, inclusion of Coulomb correlation via CAS-SCF does not alter the relative stability of the Al_2 terms, so the relative term stabilities can be understood purely based on Fermi correlation (Pauli exclusion principle). This leads to a simple description based on the bond structures of the different terms, i.e., the nodal structure of the wavefunction. Al_2 has $3p\sigma_g$ and $3p\pi_u$ bonding orbitals, and for the spin-singlet and spin-triplet terms, the most stable Ξ term has an occupied $3p\sigma_g$ orbital, i.e., the least node configuration. The stability of the spin-triplet $^3\Pi_u$ against the spin-singlet $^1\Sigma_g^+$ term also follows from HF theory. Starting from the nodeless $^1\Sigma_g^+$ wavefunction, moving one electron from the $3p\sigma_g$ into a $3p\pi_u$ with parallel spin (forming the $^3\Pi_u$ term) lowers the total energy in three steps: (i) for fixed orbitals and Al–Al bond length, V_{ee} is lowered for spin parallel electrons[35]; (ii) relaxing the electronic orbitals lowers the total energy further; and (iii) relaxing the Al–Al bond length lowers the total energy further still. Repeating steps (ii) and (iii) obviously keeps lowering the total energy until convergence is found; these steps can be roughly associated to changes in V_{en} and V_{nn}, respectively, but as seen in Fig. 1, for Al_2 V_{ee} and V_{nn} actually increase despite the initial lowering of V_{ee} in step (i). For the Ξ terms we find that for a given spin multiplicity, the total energy increases as the number of nodes in the wavefunction increases.

Coulomb correlation and bond structure. The above discussion fails for Al_3. Inclusion of Coulomb correlation via CAS-SCF un-stabilizes the spin-quadruplet terms despite their possession of two electrons in $3p\sigma$ type orbitals (a_1 and b_2 for $^4A_2$ and two a_1s for $^4B_1$) on the Al_3 molecular plane. We analyze the effects of Coulomb correlation based on the electron density distribution change defined by

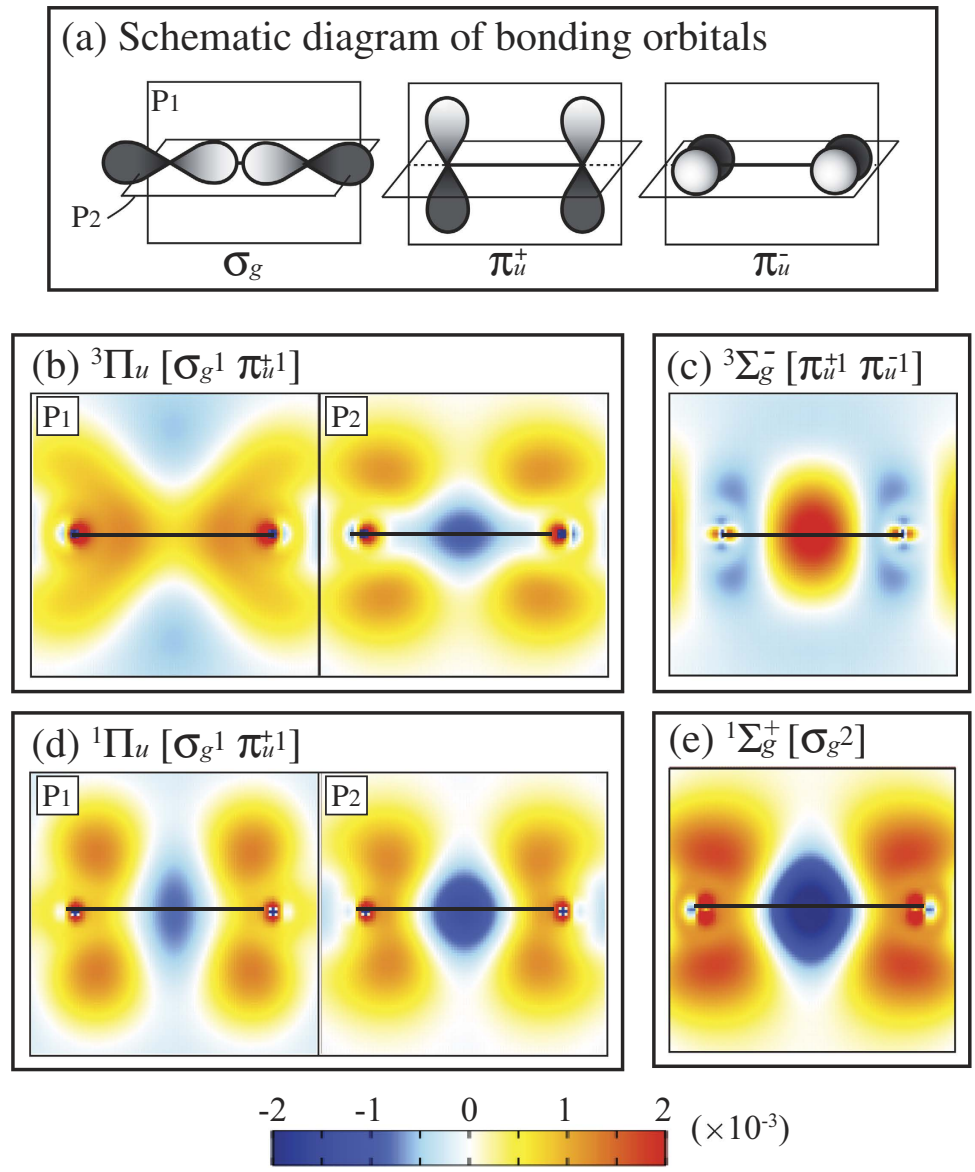

Figure 2. Schematic of bonding orbitals (**a**) and Coulomb correlation induced electron density distribution change ρ^c for stationary states of Al_2 (**b–e**).Here $\rho^c = \rho^{CAS} - \rho^{HF}$, where ρ^{CAS} is evaluated at CAS(6, 18).

$\rho^c = \rho^{CAS} - \rho^{HF}$, where ρ^{CAS} and ρ^{HF} are the total electron densities calculated by CAS-SCF and HF, respectively. The crucial Coulomb correlation that alters the Al_3 term stabilities occurs at CAS(9, 12), and therefore we evaluate ρ^{CAS} for Al_2 and Al_3 using CAS(6, 18) and CAS(9, 12), respectively. The ρ^c shown in Figs 2 and 3 for Al_2 and Al_3, respectively, are evaluated at the equilibrium nuclear configurations obtained by CAS(6, 18) and CAS(9, 12), respectively.

Al_2. The Coulomb correlation effects are analyzed based on the bonding $3p\sigma_g$ and $3p\pi_u$ orbitals shown in panel (a) of Fig. 2. Panels (b)–(e) of Fig. 2 show the electron density differences ρ^c for the $^3\Pi_u$, $^3\Sigma_g^-$, $^1\Pi_u$, and $^1\Sigma_g^+$ terms in the planes P_1 and P_2 corresponding to the $3p\sigma_g$ and $3p\pi_u$ bonding orbitals. The blue areas indicate a depletion of electron density, and the yellow–orange–red areas an increase of electron density. For the $^{3,1}\Sigma_g^\pm$ terms, these P_1 and P_2 planes are equivalent. The ρ^c analysis is omitted for the $^1\Delta_g$ term, which is not correctly represented in the HF calculation.

The CAS(6, 18) calculation includes various configurations including up to 3*d* orbitals, but the essence of the Coulomb correlation effects can be described based on the mixing of the bonding $3p\sigma_g$ and $3p\pi_u$ orbitals. As shown in panels (b)–(e) of Fig. 2, the electron density distribution corresponding to orbitals occupied in HF theory (Table 2) is depleted, and increases corresponding to bonding orbitals not occupied in HF theory. For the $^3\Pi_u$, $^1\Pi_u$, and $^1\Sigma_g^+$ terms that in HF have an occupied $3p\sigma_g$ orbital, there is a

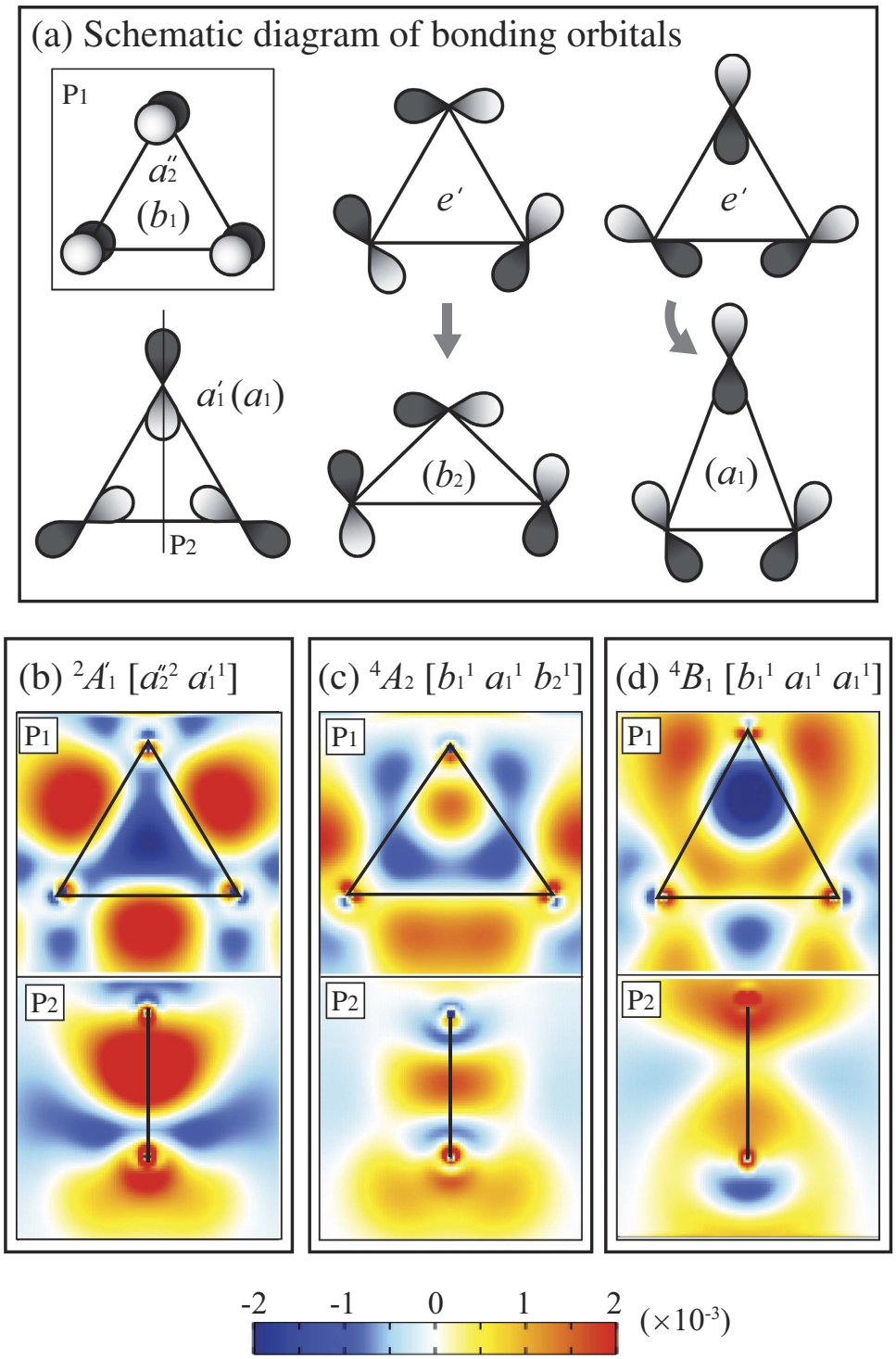

Figure 3. Schematic of bonding orbitals (**a**) and Coulomb correlation induced electron density distribution change ρ^c for stationary states of Al_3 (**b–d**). Here ρ^{CAS} is evaluated at CAS(9, 12).

depletion in ρ^c along the bond axis, and for the $^3\Sigma_g^-$ that in HF does not have an occupied $3p\sigma_g$ orbital, there is an increase. Likewise, ρ^c is negative in the regions corresponding to $3p\pi_u$ orbitals occupied in HF theory, and positive in the regions where the $3p\pi_u$ orbitals are not occupied in HF theory. Because all these Coulomb correlation effects essentially occur among the same set of orbitals, all of which are bonding, the effects are similar. Because the Coulomb correlation effects are similar for all terms, Coulomb correlation does not alter the relative stability of them, and the discussion above of term stability based on Fermi correlations and wavefunction nodal structure is sufficient.

Al_3. Al_3 has the $^2A_1'$ low-spin ground state, against expectations from Hund's first rule or the spin-state stabilization mechanism for Al_2 pertaining to HF theory. Thus, the energy lowering effect of Coulomb correlations is different for the low-spin $^2A_1'$ term and the high-spin $^4A_2$ and $^4B_1$ terms. The effect of these Coulomb correlations is discussed based on the $3p\sigma$ and $3p\pi$ orbitals shown in panel (a) of Fig. 3. Panels (b)–(d) of Fig. 3 show the electron density differences ρ^c for the $^2A_1'$, $^4A_2$, and $^4B_1$ terms in the plane P_1 of the nuclei of Al_3, and its perpendicular plane P_2, which is a reflection symmetry plane of Al_3. Notice that the nuclei of the spin-doublet $^2A_1'$ term form equilateral triangle, whereas the spin-quadruplet terms $^4A_2$ and $^4B_1$ correspond to isosceles triangles. Ensuingly, the bonding orbitals for the low-spin and high-spin terms are quite different.

$^2A_1'$ has a doubly occupied $a_{2''}$ bonding orbital, a singly occupied $a_{1'}$ orbital, and a doubly degenerate e' LUMO. The $a_{1''}$ orbital is a π bond where the plane of nuclei is a nodal plane, and the $a_{1'}$ is a σ bond with the charge density lobe in the center of the triangle. Both $a_{2''}$ and $a_{1'}$ orbitals have C_{3v} symmetry, resulting in an equilateral trimer with D_{3h} symmetry. The doubly degenerate e' LUMO corresponds to a σ bond with charge density lobes at all three sides of the triangle. The main Coulomb correlation effect is similar to what was discussed above for Al_2. There is a depletion of electron in the regions corresponding to the $a_{2''}$ and $a_{1'}$ orbitals occupied in HF theory, and an increase in the region corresponding to the e' orbitals, as seen in Fig. 3(b).

For the spin-quadruplet terms one of the $a_{2''}$ electrons occupies either one of the e' orbitals. Individually these orbitals have the C_{2v} symmetry, yielding Jahn-Teller distorted isosceles triangles as described in Table 2. This changes the also symmetry species of the occupied $a_{2''}$ and $a_{1'}$ orbitals into b_1 and a_1, respectively, but these orbitals still maintain their nature as π and σ bonds with similar charge density lobes as described above for the equilateral triangle. The newly formed a_1 or b_2 orbitals for the $^4B_1$ or $^4A_2$ terms, have charge density lobes at the base or legs of the triangle, respectively, as shown in Fig. 3(a). The LUMO of the $^4B_1$ and $^4A_2$ terms are b_2 and a_1, respectively, i.e., the other one of the e' orbitals for an equilateral triangle. For the spin-quadruplet terms, the main Coulomb correlation effect is the mixing of the a_1 or b_2 orbitals, which can be seen Fig. 3(c,d) as a depletion of electron density along the legs (base) of the triangle for $^4A_2$ ($^4B_1$) and the corresponding along the base (legs) of the triangle.

Because of different symmetries, the Coulomb correlations for the low-spin and the high-spin terms of Al_3 are fundamentally different. For the spin-doublet term, the main Coulomb correlation is the mixing of two occupied states and an unoccupied *doubly degenerate* state, whereas for the spin-quadruplet terms, the main Coulomb correlation is due to the mixing of one occupied and one unoccupied state. Coulomb correlation acts strongly among states nearby in energy and real space, and for the spin-quadruplet terms, the Jahn-Teller distortion imposes a severe limitation on the availability of such *nearby* states for mixing. This, combined with the fact that Coulomb correlation (even without geometrical distortions) is larger for low-spin configurations[2] in total stabilizes the Al_3 low-spin ground state. Thus, both Hund's first rule and the mechanism that stabilizes the high-spin ground state of Al_2 are violated because the breaking of symmetry of the Al_3 spin-quadruplet configurations reduces their Coulomb correlation. Note that Hund's maximum spin multiplicity rule is violated under exactly the opposite conditions as postulated by Kutzelnigg and Morgan[20].

Larger clusters. Application of the term rules described above for other clusters is straight forward. We illustrate this generalization by predicting ground state terms for Al_4 and Al_5. For both clusters, we consider previously described planar and pyramidal structures[26,28,38]; incidentally, our discussion below offers a new interpretation for why planar geometries are favored against pyramidal ones[39]. We predict $^3B_{1u}$ and $^2B_1$ ground states for Al_4 and Al_5, respectively, well in agreement with previous works[21,26,28]. The structures and spin multiplicities agree also with density-functional calculations[29,38], which however give no information of the symmetry species Ξ.

Al_4. Al_4 can have spin-singlet, spin-triplet, and spin-quintet states due to different configurations of four $3p$ electrons, shown in Table 3. The HOMO of any of the Al_4 terms with pyramidal structure (3-fold degenerate $2t_1$ orbitals) do not form σ-type bonds, so for any spin multiplicity, the least node wavefunctions corresponds to a planar geometry. The planar Al_4 spin-quintet terms (high spin) always have at least one occupied antibonding molecular orbital, such as $2b_{3u}$, $2b_{2u}$, $2b_{3g}$, and $2b_{2g}$, whereas the spin-triplet and singlet terms $^3B_{1u}$, ^3A_u, $^3B_{1g}$, and ^1A_g have valence electrons occupying in bonding orbitals ($1b_{1g}$, $1b_{1u}$, and $3a_g$). Thus, Fermi correlation stabilizes the spin-triplet terms with possession of most-occupied σ-type bonding orbitals, i.e., $^3B_{1u}$ state. Coulomb correlation, which enhances the electron density on the nodal plane of HOMO(s), makes Al-Al bonds on the molecular plane stronger for both $^3B_{1u}$ and ^1A_g states. As seen in stability of Al_2's spin triplet terms, such Coulomb correlation effect cannot reverse the relative stability for $^3B_{1u}$ and ^1A_g, and thus we predict $^3B_{1u}$ as the ground state term of Al_4.

Al_5. Al_5 can have spin multiplicities up to spin-sextet due to different configurations of five $3p$-electrons. All pyramidal, and the planar spin-sextet terms have at least one electron in antibonding or nonbonding orbitals (see Table 4), and thus cannot be more stable than the planar spin-doublet or spin-quadruplet terms. The planar spin-quadruplet terms (intermediate spin state) only have partial bonds, such as $3b_1$,

Geometry	Electronic configuration		Schematic molecular orbitals
Planar	$^5B_{3g/2g}$	$[3s]\ 1b_{1g}^1\ 1b_{1u}^1\ 3a_g^1\ 2b_{3u/2u}^1$	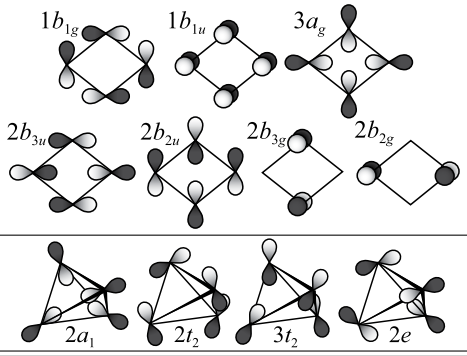
	$^5B_{3u/2u}$	$[3s]\ 1b_{1g}^1\ 1b_{1u}^1\ 3a_g^1\ 2b_{3g/2g}^1$	
	$^3B_{1u}$	$[3s]\ 1b_{1g}^2\ 1b_{1u}^1\ 3a_g^1$	
	^3A_u	$[3s]\ 3a_g^2\ 1b_{1g}^1\ 1b_{1u}^1$	
	$^3B_{1g}$	$[3s]\ 1b_{1u}^2\ 1b_{1g}^1\ 3a_g^1$	
	^1A_g	$[3s]\ 1b_{1g}^2\ 1b_{1u}^2$	
Pyramidal	$^5A_1$	$[3s]\ 2a_1^1\ 2t_2^3$	
	$^3T_1$	$[3s]\ 2a_1^2\ 2t_2^2$	
	$^1T_1$	$[3s]\ 2a_1^2\ 2t_2^2$	

Table 3. Electronic configurations of valence electrons for planar and pyramidal geometries for Al_4. Here $[3s]=1a_g^2\ \ 1b_{3u}^2\ \ 1b_{2u}^2\ \ 2a_g^2$ for the planar, and $[3s]=1a_1^2\ \ 1t_2^6$ for the pyramidal geometries.

Geometry	Electronic configuration		Schematic molecular orbitals
Planar	$^4A_1$	$[3s]\ 2b_1^2\ 1b_2^2\ 4a_1^1\ 3b_1^1\ 4b_1^1$	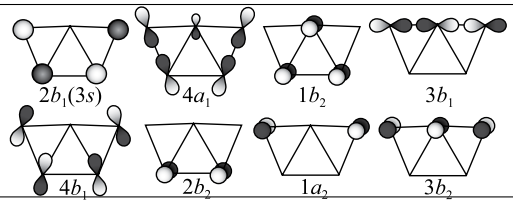
	$^4A_2$	$[3s]\ 1b_2^2\ 1a_2^2\ 4a_1^1\ 2b_1^1\ 2b_2^1$	
	$^2B_1$	$[3s]\ 2b_1^2\ 1b_2^2\ 4a_1^2\ 3b_1^1$	
	$^2B_2$	$[3s]\ 1b_2^2\ 1b_1^2\ 2a_1^2\ 2b_2^1$	
	$^2A_1$	$[3s]\ 2b_1^2\ 1b_2^2\ (3b_1/2b_2)^2\ 4a_1^1$	
Pyramidal	$^4A_1$	$[3s]\ 1b_2^2\ (3a_1/4a_1)^1\ (2e/3e)^2$	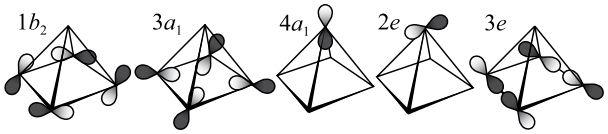
	^4E	$[3s]\ 1b_2^2\ 3a_1^1\ 4a_1^1\ (2e/3e)^1$	
	^2E	$[3s]\ 1b_2^2\ 3a_1^2\ 2e^1$	
	$^2A_1$	$[3s]\ 2b_1^2\ 1b_2^2\ (3b_1/2b_2)^2\ 4a_1^1$	

Table 4. Electronic configurations of valence electrons for planar and pyramidal geometries for Al_5. Here $[3s]=1a_1^2\ \ 1b_1^2\ \ 2a_1^2\ \ 3a_1^2$ for the planar, and $[3s]=1a_1^2\ \ 1e_1^4\ \ 2a_1^2\ \ 1b_1^2$ for the pyramidal geometries.

$4b_1$, and $2b_2$, which leaves only spin-doublet terms with strong σ-type bonds. Thus for Al_5, we predict the planar $^2B_1$ spin-doublet term, which has the least node structure ground state.

Discussion

Our benchmark first principles calculation predicts the $^3\Pi_u$ (high-spin) and $^2A_1'$ (low-spin) ground states for Al_2 and Al_3, respectively. Detailed analysis of potential energy components of the total energy reveal that previous interpretations, attributing atomic or molecular term stabilization to either V_{ee}[35,36] or V_{en}[2,5,8] are, in general, not valid for multi-atom systems. The relative stability of the Ξ terms for a given spin multiplicity for either Al_2 and Al_3 follows simple arguments based on bonding structures: For a given spin multiplicity the Ξ term possessing the most-occupied σ bonding orbitals (least node structure) is stabilized within the one-electron orbital picture according to Hartree-Fock (HF) theory. In addition, HF theory tends to stabilize the high-spin term due to Fermi correlation (Pauli exclusion principle). Coulomb correlation lowers the energy by mixing some of the orbitals occupied in HF theory with nearby unoccupied orbitals. For Al_2, the Coulomb correlation effects are similar for all terms, but for Al_3, Coulomb correlation alters the relative term stability. For Al_3, breaking of symmetry of the the spin-quadruplet terms significantly limits the orbital mixing and energy lowering by Coulomb correlation. The high symmetry of the spin-doublet term, on the other hand, allows for mixing with *degenerate* levels followed by a much larger energy lowering by Coulomb correlation, stabilizing the low-spin $^2A_1'$ ground state of Al_3. These stabilization mechanisms are not specific for Al clusters, and serve as simple term rules to determine the ground state of arbitrary multi-atomic systems. We demonstrate this predictive power by predicting $^3B_{1u}$ and $^2B_1$ ground states for Al_4 and Al_5, respectively.

Methods

The total energy E of the $^{2S+1}\Xi g/u$ term of an Al_n cluster in the Born-Oppenheimer approximation is given by $\left\langle {}^{2S+1}\Xi g/u \middle| \hat{T} + \hat{V}_{nn} + \hat{V}_{en} + \hat{V}_{ee} \middle| {}^{2S+1}\Xi g/u \right\rangle$, where $\left| {}^{2S+1}\Xi g/u \right\rangle$ is a many-electron wavefunc-

tion and the operators $\hat{O}$ give the electron kinetic energy, the inter-nuclear repulsion, the electronuclear attraction, and the inter-electron repulsion, respectively. The expectation values $\left\langle {}^{2S+1}\Xi g/u \middle| \hat{O} \middle| {}^{2S+1}\Xi g/u \right\rangle$ for each operator $\hat{O}$, henceforth denoted as $O({}^{2S+1}\Xi g/u)$, are calculated using the GAMESS package[40]. We use both Hartree-Fock (HF) method and complete active space self-consistent field (CAS-SCF) method. Our CAS-SCF many-electron wavefunctions contain configuration interactions among the 3*s* and 3*p* valence shells and empty 3*d*-derived orbitals: CAS(6, 26) and CAS(9, 18) for Al_2 and Al_3, respectively. CAS(n, m) stands for a CAS-SCF calculation with *n* active spaces and *m* active electrons. Atomic orbitals are expanded within the aug-cc-pVTZ basis set, and all nuclear positions are relaxed. This gives a virial ratio of $-V/T = 2.00000 \pm 0.00003$ for each molecular term ${}^{2S+1}\Xi g/u$.

References

1. Hund, F. Zur Deutung verwickelter Spektren, insbesondere der Elemente Scandium bis Nickel. *Z. Physik* **33,** 345–371 (1925).
2. Katriel, J. & Pauncz, R. Theoretical interpretation of Hund's rule. *Adv. in Quantum Chem.* **10,** 143–185 (1977).
3. Boyd, R. J. A quantum mechanical explanation for Hund's multiplicity rule. *Nature* **310,** 480–481 (1984).
4. Darvesh, K. V., Fricker, P. D. & Boyd, R. J. Interpretation of Hund's rule for first-row hydrides AH (A = Li, B, N, F). *J. Chem. Phys.* **94,** 3480–3484 (1990).
5. Oyamada, T., Hongo, K., Kawazoe, Y. & Yasuhara, H. Unified interpretation of Hund's first and second rules for 2*p* and 3*p* atoms. *J. Chem. Phys.* **133,** 164113 (2010).
6. Tanaka, K., Nomura, T. & Noro, T. Ab initio SCF CI calculations on the ground and π-π* excited states of the pyrrole molecule and its positive ion. *J. Chem. Phys.* **67,** 5738–3741 (1977).
7. Darvesh, K. V. & Boyd, R. J. Hund's rule and singlet-triplet energy differences for the lowest $n\pi^*$ states of formaldehyde, H_2CO. *J. Chem. Phys.* **90,** 5638–5643 (1989).
8. Maruyama, Y., Hongo, K., Tachikawa, M., Kawazoe, Y. & Yasuhara, H. Ab initio interpretation of Hund's rule for the methylene molecule: Variational optimization of its molecular geometries and energy component analysis. *Int J Quantum Chem* **108,** 731–743 (2008).
9. Slipchenko *et al.* 5-Dehydro-1,3-quinodimethane: A Hydrocarbon with an Open-Shell Doublet Ground State. *Angew Chem Int Edit* **43,** 742–745 (2004).
10. Fumi, F. G. & Parr, R. G. Electronic States of Diatomic Molecules: The Oxygen Molecule. *J. Chem. Phys.* **21,** 1864 (1953).
11. Padgett, A. A. & Griffing, V. LCAO-MO SCF Study of B2. *J. Chem. Phys.* **30,** 1286 (1959).
12. Bender, C. F. & Davidson, E. R. Electronic Structure of the B2 Molecule. *J. Chem. Phys.* **46,** 3313–3319 (1967).
13. Yoshimine, M. The second ${}^3\Sigma_u^-$ state of O_2. *J. Chem. Phys.* **64,** 2254 (1976).
14. Stevens, W. J. & Krauss, M. The electronic structure of the ground and excited states of Mg_2^+ and Mg_2. *J. Chem. Phys.* **67,** 1977 (1977).
15. Tatewaki, H. *et al.* Configuration-Interaction study of lower excited states of O_2: Valence and Rydberg characters of the two lowest ${}^3\Sigma_u^-$ states. *Int. J. Quantum Chem.* **15,** 533–545 (1979).
16. Delyagina, I. A., Kokh, D. B. & Pravilov, A. M. Study of the covalent and triplet ionic-pairing states of the fluorine molecule with the MRDCI method. *Optics and Spectroscopy* **94,** 170–178 (2003).
17. Bytautas, L., Matsunaga, N., Nagata, T., Gordon, M. S. & Ruedenberg, K. Accurate ab initio potential energy curve of F_2. II. Core-valence correlations, relativistic contributions, and long-range interactions. *J. Chem. Phys.* **127,** 204301 (2007).
18. Su, P. *et al.* Bonding Conundrums in the C_2 Molecule: A Valence Bond Study. *J. Chem. Theory Comput.* **7,** 121–130 (2011).
19. Magoulas, I., Kalemos, A. & Mavridis, A. An ab initio study of the electronic structure of BF and BF^+. *J. Chem. Phys.* **138,** 104312 (2013).
20. Kutzelnigg, W. & Morgan, J. D. III. Hund's rules. *Z Phys D* **36,** 197–214 (1996).
21. Pacchioni, G., Plavšić, D. & Koutecký, J. Chemical bonding and electronic structure of small homonuclear clusters of elements of groups IA, IIA, IIIA and IVA. *Ber. Bunsenges. Phys. Chem.* **87,** 503–512 (1983).
22. Pacchioni, G. & Koutecký, J. Silicon and germanium clusters. A theoretical study of their electronic structures and properties. *J. Chem. Phys.* **84,** 3301–3310 (1986).
23. Pacchioni, G. & Koutecký, J. Ab initio MRD CI investigation of the optical spectra of C_4 and C_5 clusters. *J. Chem. Phys.* **88,** 1066–1073 (1988).
24. Zabala, N., Puska, M. J. & Nieminen, R. M. Spontaneous magnetization of simple metal nanowires. *Phys. Rev. Lett.* **80,** 3336–3339 (1998).
25. Ayuela, A., Raebiger, H., Puska, M. & Nieminen, R. Spontaneous magnetization of aluminum nanowires deposited on the NaCl(100) surface. *Phys. Rev. B* **66,** 035417 (2002).
26. Pettersson, L., Bauschlicher, C. W. & Halicioglu, T. Small Al clusters. II. Structure and binding in Al_n ($n = 2$-6, 13). *J. Chem. Phys.* **87,** 2205–2213 (1987).
27. Bauschlicher, C. W., Partridge, H., Langhoff, S. R., Taylor, P. R. & Walch, S. P. Accurate ab initio calculations which demonstrate a ${}^3\Pi_u$ ground state for Al_2. *J. Chem. Phys.* **86,** 7007–7012 (1987).
28. Meier, U., Peyerimhoff, S. D. & Grein, F. Ab initio MRD-CI study of neutral and charged Ga_2, Ga_3 and Ga_4 clusters and comparison with corresponding boron and aluminum clusters. *Z. Physik D Atom. Mol. Cl.* **17,** 209–224 (1990).
29. Rao, B. K. & Jena, P. Evolution of the electronic structure and properties of neutral and charged aluminum clusters: A comprehensive analysis. *J. Chem. Phys.* **111,** 1890–1904 (1999).
30. Cox, D. M., Trevor, D. J., Whetten, R. L., Rohlfing, E. A. & Kaldor, A. Aluminum clusters: Magnetic properties. *J. Chem. Phys.* **84,** 4651–4656 (1986).
31. Howard, J. A., Sutcliffe, R., Tse, J. S., Dahmane, H. & Mile, B. Electron spin resonance spectra of the aluminum trimer in hydrocarbon matrices: A quartet ${}^4A_2$ state. *J. Phys. Chem.* **89,** 3595–3599 (1985).
32. Tse, J. S. Stability and potential energy surface of the three low lying electronic states of Al_3. *J. Chem. Phys.* **92,** 2488–2494 (1990).
33. Hamrick, Y. M., Vanzee, R. J. & Weltner, W. Electron-spin resonance and ground states of the boron and aluminum trimers. *J. Chem. Phys.* **96,** 1767–1775 (1992).
34. Cai, M. F., Dzugan, T. P. & Bondybey, V. E. Fluorescene studies of laser vaporized aluminum: Evidence for a ${}^3\Pi_u$ ground state of aluminum dimer. *Chemical Physics Letters* **155,** 430–436 (1989).
35. Slater, J. C. The theory of complex spectra. *Phys. Rev.* **34,** 1293–1322 (1929).
36. Van Vleck, J. H. Valence strength and the magnetism of complex salts. *J. Chem. Phys.* **3,** 807 (1935).
37. Colpa, J. P. & Brown, R. E. The inequality formulation of Hund's rule and a reinterpretation of singlet–triplet energy differences, generalized for molecules at equilibrium geometry. *J. Chem. Phys.* **68,** 4248–4251 (1978).
38. Jones, R. O. Structure and bonding in small aluminum clusters. *Phys. Rev. Lett.* **67,** 224 (1991).

39. Geske, G. D., Boldyrev, A. I., Li, X. & Wang, L.-S. On the origin of planarity in Al_5^- and Al_5 clusters: The importance of a four-center peripheral bond. *J. Chem. Phys.* **113,** 5130 (2000).
40. Schmidt, M. W. *et al.* General atomic and molecular electronic structure system. *J. Comput. Chem.* **14,** 1347–1363 (1993).

Acknowledgements

This paper is dedicated to the memory of Professor H. Yasuhara, who was an inspiring mentor during the initial stages of this work. The authors thank S. Fukutomi, K. Hongo, Y. Kawazoe, Y. Kita, Y. Maruyama, U. Nagashima, T. Oyamada, and M. Tachikawa for discussions. H.R. thanks for financial support from Brazilian funding agency FAPESP.

Author Contributions

D.Y. conducted the calculations, D.Y. and H.R. analysed the results. H.R. wrote the manuscript. Both authors reviewed the manuscript.

Additional Information

Competing financial interests: The authors declare no competing financial interests.

How to cite this article: Yoshida, D. and Raebiger, H. Term rules for simple metal clusters. *Sci. Rep.* **5**, 15760; doi: 10.1038/srep15760 (2015).